value to workers wishing to study the reactivity and applications of this class of compounds. However, the details of our X-ray crystallographic structure determination of **4** do not provide a convincing basis for explaining the carbene-like reactivity of this compound. Further investigations are in progrss in our laboratory to probe the mechanistic features of the reactions of **4** and related compounds.

Acknowledgment. We are grateful to Professor Joseph W. Lauher of this department for providing assistance in the X-ray structure determination, to Professor Robert C. Kerber, also of this department, for valuable discussions, and to the donors of the Petroleum Research Fund, administered by the American Chemical Socity (Grant No. 12032-AC1,3), and the National Science Foundation (Grant No. CHE 7918019) for providing the financial support for this investigation.

Registry No. 4, 80679-39-6; $[(\eta^5\text{-}C_5H_5)Fe(CO)_2]_2$, 12154-95-9.

Supplementary Material Available: Tables of crystal data, scattering factors, bond distances and bond angles, positional and thermal parameters, and calculated and observed structure factor amplitudes (14 pages). Ordering information is given on any current masthead page.

Synthesis, Molecular Structure, and Reactions of Bis(tetraphenylphosphonium) Hexakis(μ-thiophenolato)-tetrachlorotetraferrate(II), $(Ph_4P)_2[Fe_4(SPh)_6Cl_4]$. Its Reactions with Dibenzyl Trisulfide and the Synthesis of the $[Fe_4S_4Cl_4]^{2-}$ and $[Fe_4S_4(Cl)_2(SC_6H_5)_2]^{2-}$ "Cubane"-Type Clusters

D. Coucouvanis,* M. Kanatzidis, E. Simhon, and N. C. Baenziger

Contribution from the Department of Chemistry, University of Iowa, Iowa City, Iowa 52242.

Received August 24, 1981

Abstract: The reaction between $FeCl_2$, $(C_6H_5)_4PCl$, and KSC_6H_5 in acetonitrile in at 2:1:3 molar ratio or between $[Fe(SC_6H_5)_4]^{2-}$ and FeX_2 (X = Cl, Br) in a 1:2.4 molar ratio affords in excellent yields the new $[Fe_4(SC_6H_5)_6X_4]^{2-}$ clusters. The paramagnetic $[(C_6H_5)_4P]_2[Fe_4(SC_6H_5)_6Cl_4]$ (I) crystallizes in the triclinic space group $P\bar{1}$ with two molecules in the unit cell. The cell dimensions are $a = 23.122$ (6) Å, $b = 13.986$ (1) Å, $c = 14.189$ (4) Å, $\alpha = 73.65$ (1)°, $\beta = 80.58$ (1)°, and $\gamma = 84.91$ (1)°. Intensity data were collected with a four-circle computer-controlled diffractometer with use of the θ–2θ step scan technique. All of the nonhydrogen atoms in the anion and the two phosphorus atoms in the cations were refined with anisotropic temperature factors while the carbon atoms in the $(C_6H_5)_4P^+$ cations were refined with isotropic temperature factors. Refinement by full-matrix least squares of 661 parameters on 5514 data gave a final R value of 0.074. The hydrogen atoms were included in the structure factor calculation but were not refined. The overall description of the $Fe_4S_6Cl_4$ core in I is that of a nearly regular Fe_4 tetrahedron inscribed in a slightly irregular octahedron defined by the bridging S atoms in an "adamantane" type of cage. The four chlorine atoms coordinated one on each of the four iron atoms define an outer tetrahedron such that the overall symmetry of the $Fe_4S_6Cl_4$ unit is very nearly T_d. Average values of selected structural parameters and the estimated standard deviations calculated from scatter of values around the mean are Fe–Fe = 3.94 (4) Å, Fe–S = 2.362 (15) Å, Fe–Cl = 2.254 (3) Å, S–S = 3.79 (2) Å, S–Cl = 3.82 (7) Å; Fe–Fe–Fe = 60 (1)°, Fe–S–C = 108.3 (25), Cl–Fe–S = 112 (3), S–Fe–S = 107 (7)°, Fe–S–Fe = 113 (2)°. Distortions in each of the four tetrahedral $ClFe^{II}S_3$ units can be explained in terms of phenyl ring repulsions on the periphery of the Fe_4S_6 cage. The reactions of dibenzyl trisulfide with I in ratios that do not exceed 2, in either CH_3CN or $CH_3CN/HCON(CH_3)_2$ mixtures, afford the new mixed ligand "cubane" $[(C_6H_5)_4P]_2[Fe_4S_4(SC_6H_5)_2Cl_2]$ (II) in very good yields. The chemical and physical properties including electrochemical properties and proton magnetic resonance spectra as well as preliminary X-ray crystallographic results confirm the identity of II. In reactions where the dibenzyl trisulfide to I ratio exceeds 4, the $[Fe_4S_4Cl_4]^{2-}$ (III) "cubane"-type cluster forms and can be isolated in excellent yields when the reagent ratio is 8:1.

Interest in the fundamental coordination chemistry of simple thiolate ligands derives to a great extent from recent advances in the chemistry of metalloproteins. The importance of thiolate coordination in the metal sites of these proteins has been demonstrated in numerous crystallographic studies.[1] Outstanding among the metalloproteins which have been studied in detail are the various types of ferredoxins.[2] In these electron transfer, nonheme iron proteins, thiolato groups of protein-bound cysteinyl residues serve as coordination anchor points for such inorganic cores as Fe_4S_4,[3] Fe_3S_3,[4] or Fe_2S_2[5] and for single Fe(II) or Fe(III)[1a] ions.

Significant recent accomplishments in metal thiolate coordination chemistry include (a) the synthesis and detailed characterization of the $Fe_4S_4(SR)_4$, $Fe_2S_2(SR)_4$, and $Fe(SR)_4$ complexes in various oxidation levels,[6] (b) the synthesis[7] and structural

---

(1) (a) Watenpaugh, K. D.; Sieker, L. C.; Herriott, J. R.; Jensen, L. H. *Acta Crystallogr., Sect. B* **1973**, *B29*, 943. (b) Jensen, L. H. In "Iron-Sulfur Proteins"; Lovenberg, W., Ed.; Academic Press: New York, 1973; Vol. II, Chapter 4. (c) Eklund, H.; Nordström, B.; Zeppezauer, E.; Soderlund, G.; Ohlesson, I.; Boiwe, T.; Brånden, C. I. *FEBS Lett.* **1974**, *44*, 200. (d) Eklund, H.; Nordstrom, B.; Zeppezauer, E.; Soderlund, G.; Ohlesson, I.; Boiwe, T.; Soderberg, B. O.; Tapia, O.; Brånden, C. I. *J. Mol. Biol.* **1976**, *102*, 27. (e) Adman, A. T.; Sieker, L. C.; Jensen, L. H. *J. Biol. Chem.* **1973**, *248*, 2987.

(2) (a) Orme-Johnson, W. H. *Annu. Rev. Biochem.* **1973**, *42*, 159. (b) Lovenberg, W., Ed. "Iron-Sulfur Proteins"; Academic Press: New York, 1977; Vol. III. (c) Averill, B. A. Orme-Johnson, W. H. In "Metal Ions in Biological Systems"; Sigel, H., Ed., Marcel Dekker: New York, 1978; Vol. 7.

(3) Freer, S. T.; Alden, R. A.; Carter, C. W.; Kraut, J. *J. Biol. Chem.* **1975**, *250*, 46.

0002-7863/82/1504-1874$01.25/0

characterization[8] of monomeric, tetrahedral $[M(SPh)_4]^{2-}$ complexes [M = Mn, Fe, Co, Ni, Zn, Cd] with the thiophenolate (PhS^-) ligand, and (c) certain polynuclear thiophenolate complexes of the type $[M_4(SPh)_yL_z]^{2-}$ (M = Co, $y = 10$, $z = 0$;[9] M = Fe, $y = 10$, $z = 0$;[10] M = Zn, $y = 8$, L = Cl, $z = 2$;[11] M = Cu, $y = 6$, $z = 0$[12,13]) and of the catenated $Zn_4(SPh)_8(CH_3OH)$ cluster[14] which possess as a common characteristic the $M_4(\mu\text{-}SPh)_6$ "adamantane" cores.

Upon recognition of the $[Fe(SPh)_4]^{2-}$ complex as a reducing, coordinatively unsaturated anion, we proceeded with a study of the specific oxidative addition reactions of this complex with organic trisulfides (RSSSR). The choice of trisulfides as oxidizing agents was based on the expectation that upon reduction, the trisulfides would generate S^{2-} which might be incorporated in the iron-containing oxidation products. These expectations were fulfilled to the extent that the oxidation of $[Fe(SPh)_4]^{2-}$ with dibenzyl trisulfide in a homogeneous solution resulted in the high-yield syntheis of the $[Fe_2S_2(SPh)_4]^{2-}$ complex.[15] Subsequent to this study, which we proposed to be potentially important in understanding the biosynthesis of ferredoxins, a very similar oxidation of $[Fe(SPh)_4]^{2-}$ with elemental sulfur was reported[16] to produce $[Fe_2S_2(SPh)_4]^{2-}$. This last reaction and the use of elemental sulfur were foreshadowed by the synthetic studies of Christou and Garner, who showed that in the presence of excess thiolate and sulfur, Fe(II) or Fe(III) salts afforded the $[Fe_4S_4(SR)_4]^{2-}$ clusters.[17]

In this paper we describe the synthesis and molecular structure of $[Fe_4(SPh)_6Cl_4]^{2-}$, a new cluster containing the $Fe_4(SPh)_6$ adamantane core. As a continuation of our studies on the oxidation of iron thiolate complexes with aliphatic trisulfides, we have studied the reactions of the $[Fe_4(SPh)_6Cl_4]^{2-}$ cluster with dibenzyl trisulfide.

These reactions allowed for the convenient, high-yield syntheses of the $[Fe_4S_4(Cl)_2(SPh)_2]^{2-}$ and $[Fe_4S_4Cl_4]^{2-}$ cubane-type clusters. To our knowledge the former has not been isolated previously and may prove useful in the synthesis of "mixed-ligand" $Fe_4S_4(SR)_2(L)_2$ clusters, while the latter is known[18] to be a convenient general starting reagent for the synthesis of the $[Fe_4S_4(SR)_4]^{2-}$ cubanes with either aliphatic or aromatic thiolate ligands.

Experimental Section

Synthesis. The chemicals in this research were used as purchased. Dimethylformamide (DMF) was stored over 4A Linde molecular sieves for 24 h and then distilled under reduced pressure at ~30 °C. Acetonitrile (CH_3CN) was distilled from calcium hydride (CaH_2) before use. Commercial grade methylene chloride (CH_2Cl_2) was distilled from CaH_2. Absolute ethanol and diethyl ether were used without any further purification. Potassium phenyl mercaptide (KSPh) was obtained by the reaction of potassium metal with thiophenol in tetrahydrofuran under dinitrogen. With the exception of dibenzyl trisulfide (BzSSSBz) and KSPh all syntheses were carried out under a dinitrogen atmosphere in a Vacuum Atmospheres Dri-Lab glovebox. Elemental analyses on samples dried under vacuum for 12 h were performed by Galbraith Analytical Laboratories, Knoxville, TN.

Physical Methods. Visible and ultraviolet spectra were obtained on Cary Model 118 and 219 spectrophotometers. Solution near-infrared studies were conducted on a Beckman DK-2 spectrophotometer. A Debye-Scherrer camera using nickel-filtered copper radiation was utilized to obtain X-ray powder diffraction patterns. Proton NMR spectra were obtained on a JEOL FX90Q Pulse FT NMR spectrometer with Me_4Si as internal standard. Chemical shifts are reported in parts per million (ppm). The following convention is used whenever isotropically shifted NMR spectra are reported. A negative sign is assigned to a resonance appearing downfield from Me_4Si. A positive sign is given to absorptions occurring upfield from Me_4Si.

Electrochemical measurements were performed with a PAR Model 173 potentiostat/galvanostat and a PAR Model 175 universal programmer. The electrochemical cell used had platinum working and auxiliary electrodes. As reference electrode a saturated calomel electrode was used. All solvents used in the electrochemical measurements were properly dried and distilled, and tetra-*n*-butylammonium perchlorate (Bu_4NClO_4) was used as the supporting electrolyte. Normal concentrations used were ~0.001 M in electroanalyte and 0.1 M in supporting electrolyte. Purified dinitrogen was used to purge the solutions prior to the electrochemical measurements. The powder diffraction diagrams were obtained by using a 114-mm diameter Debye–Scherrer type camera with Ni-filtered Cu Kα radiation ($\lambda = 1.5418$ Å).

Preparation of Compounds. Bis(tetraphenylphosphonium) Hexakis(μ-thiophenolato)-tetrachlorotetraferrate(II), $(Ph_4P)_2[Fe_4(SPh)_6Cl_4]$. Anhydrous $FeCl_2$ (0.304 g, 2.4 mmol) was dissolved in 10 mL of hot CH_3CN and the hot solution filtered. To the clear filtrate was added a hot, filtered CH_3CN solution of 1.18 g of bis(tetraphenylphosphonium) tetrakis(thiophenolato)ferrate (II), $(Ph_4P)_2Fe(SPh)_4$[8c] (1.0 mmol) in 20 mL of CH_3CN. A green yellow solution was formed and allowed to cool to ambient temperature. After diethyl ether was added to incipient crystallization and the mixture left to stand for ca. 0.5 h the solution deposited 0.984 g of analytically pure yellow plates (87% yield based on RS^-). The crystalline product can be recrystallized from CH_3CN/diethyl ether mixtures.

Anal. Calcd for $Fe_4S_6Cl_4C_{84}H_{70}P_2$ (mol wt 1699.04): C, 59.38; H, 4.16; S, 11.32; Cl, 8.34; Fe, 13.15; P. 3.64. Found: C, 59.25; H, 4.25; S, 11.27; Cl, 7.75; Fe, 12.44; P, 3.62.

X-ray powder pattern spacings (Å): 12.55 (s), 11.10 (vs), 9.50 (vw), 8.10 (m), 7.23 (w), 6.95 (w), 4.75 (m), 4.49 (s), 4.10 (w), 3.77 (w), 3.47 (w), 3.21 (m), 2.65 (w), 2.46 (vw).

Bis(tetraphenylphosphonium) Hexakis(μ-thiophenolato)-tetrabromotetraferrate(II), $(Ph_4P)_2[Fe_4(SPh)_6Br_4]$. This complex was obtained by using anhydrous $FeBr_2$ in procedures identical with those described for the synthesis of the corresponding chloro complex. The yellow plates (1.225 g, 76% yield) show an X-ray powder pattern identical with that of $(Ph_4P)_2[Fe_4(SPh)_6Cl_4]$.

Anal. Calcd for $Fe_4S_6Br_4C_{84}H_{70}P_2$ (mol wt 1876.8): C, 53.75; H, 3.77; S, 10.25; Br, 17.03; Fe, 11.90; P, 3.30. Found: C, 52.67; H, 3.85; S, 9.73; Br, 16.18; Fe, 11.44; P, 3.24.

Dibenzyl Trisulfide ($C_6H_5CH_2SSSCH_2C_6H_5$). A solution of 24.4 mL of benzyl thiol (0.25 mol) in 75 mL of petroleum ether (30–60 °C fraction) was cooled to 0 °C in an ice bath. To this cooling solution was slowly added a solution of 8.2 mL of SCl_2 (0.125 mol) in 50 mL of petroleum ether utilizing a 100 mL pressure equalizing dropping funnel. After all the SCl_2 solution was added (~1 h), the reaction mixture was allowed to warm to ambient temperature and let stand for an additional 1 h. At this stage half of the solution was removed under reduced pressure, and the reaction container was immersed in liquid dinitrogen. When the contents were rethawed, a white solid was obtained and isolated by filtration using a Büchner funnel. The crude product was dissolved in 300 mL of boiling pentane, and the solution was stored at 0 °C for ca. 12 h. The pale yellow crystalline material was collected by filtration, washed once with cold pentane, and dried under vacuum (21.6 g, 62% yield). The mass spectrum of the product shows the presence of only $(C_6H_5CH_2)_2S_3$ and only a trace of the tetrasulfide $(C_6H_5CH_2)_2S_4$.

Bis(tetraphenylphosphonium) (Dithiophenolato)dichlorotetra-μ_3-sulfido-tetraferrate(II,III)), $(Ph_4P)_2[Fe_4S_4(SPh)_2Cl_2]$. (A) In CH_3CN **with a 1:4 $[Fe_4(SPh)_6Cl_4]^{2-}$/BzSSSBz Molar Ratio.** An amount of 0.280 g (0.16 mmol) of $(Ph_4P)_2[Fe_4(SPh)_6Cl_4]$ was dissolved in 40 mL of CH_3CN, and to the resultant solution was added a solution of 0.183 g (0.65 mmol) of BzSSSBz in 20 mL of CH_3CN with stirring. After being

---

[4] Stout, D. C.; Ghosh, D.; Pattabhi, V. Robbins, A. H. *J. Biol. Chem.* **1980**, *255*, 1797.

[5] Fukuyama, K.; Hase, T.; Matsumoto, S.; Tsukihara, T.; Katsube, Y.; Tanaka, N.; Kakudo, M.; Wada, K.; Matsubara, H. *Nature (London)* **1980**, *286*, 522.

[6] Holm, R. H. *Acc. Chem. Res.* **1977**, *10*, 427 and references therein.

[7] Holah, D. G.; Coucouvanis, D. *J. Am. Chem. Soc.* **1975**, *97*, 6917.

[8] (a) Swenson, D.; Baenziger, N. C.; Coucouvanis, D. *J. Am. Chem. Soc.* **1978**; *100*, 1932. (b) Coucouvanis, D.; Swenson, D.; Baenziger, N. C.; Holah, D. G.; Kostikas, A.; Simopoulos, A.; Petrouleas, V. *J. Am. Chem. Soc.* **1976**, *98*, 5721. (c) Coucouvanis, D.; Swenson, D.; Baenziger, N. C.; Murphy, C.; Holah, D. G.; Sfarnas, N.; Simopoulos, A.; Kostikas, A. *J. Am. Chem. Soc.* **1981**, *103*, 3350.

[9] (a) Dance, I. G.; Calabrese, J. C. *J. Chem. Soc., Chem. Comm.* **1975**, 762. (b) Dance, I. G. *J. Am. Chem. Soc.* **1979**, *101*, 6264.

[10] Hagen, K. S.; Berg, J. M.; Holm, R. H. *Inorg. Chim. Acta* **1980**, *45*, L17.

[11] Dance, I. G. *Inorg. Chem.* **1981**, *20*, 2155.

[12] Coucouvanis, D.; Murphy, C. N.; Kanodia, S. K. *Inorg. Chem.* **1980**, *19*, 2993.

[13] Dance, I. G.; Calabrese, J. C. *Inorg. Chim. Acta* **1976**, *19*, L41.

[14] Dance, I. G. *J. Am. Chem. Soc.* **1980**, *102*, 3445.

[15] Coucouvanis, D.; Swenson, D.; Stremple, P.; Baenziger, N. C. *J. Am. Chem. Soc.* **1979**, *101*, 3392.

[16] Hagen, K. S.; Reynolds, J. G.; Holm, R. H. *J. Am. Chem. Soc.* **1981**, *103*, 4054.

[17] Christou, G.; Garner, C. D. *J. Chem. Soc., Dalton Trans.* **1979**, 1093.

[18] (a) Wong, G. B.; Bobrik, M. A.; Holm, R. H. *Inorg. Chem.* **1978**, *17*, 578 and references therein. (b) Bobrik, M. A.; Hodgson, K. O.; Holm, R. H. *Inorg. Chem.* **1977**, *16*, 1851.

stirred 20 min, under N_2, the brown solution was filtered and a mixture of ethyl alcohol–diethyl ether was added to the filtrate (5 mL of EtOH, 80 mL of Et_2O). When the mixture was left standing for ca 2 h, black crystals formed and were isolated (0.185 g, 84% yield).

Anal. Calcd for $Fe_4S_6Cl_2C_{60}H_{50}P_2$ (mol wt 1319): C, 54.58; H, 3.79; P, 4.70; Fe, 16.98; S, 14.56; Cl, 5.38. Found: C, 54.10; H, 4.05; P, 4.69; Fe, 16.73; S, 14.67; Cl, 5.58.

X-ray powder pattern spacings (Åa): 10.85 (s), 9.50 (s), 7.73 (vs), 5.98 (w), 5.18 (w), 6.80 (vw), 4.85 (s), 4.40 (vw), 4.08 (s), 3.75 (m), 3.17 (vw), 3.08 (w).

(B) In DMF by the Reaction of $(Ph_4P)_2[Fe_4S_4Cl_4]$ and $(Ph_4P)_2[Fe_4S_4(SPh)_4]$ in a 1:1 Molar Ratio. An amount of 0.152 g (0.64 mmol) of $(Ph_4P)_2(Fe_4S_4Cl_4)$ in 30 mL of DMF was added to a solution of $(Ph_4P)_2[Fe_4S_4(SPh)_4]$ (0.189 g, 0.64 mmol) in 30 mL of DMF. The solution was filtered after ca. 5 min and was allowed to stand at ambient temperature for ca. 12 h. When 100 mL of diethyl ether was added to the solution and it was left to stand for 5 h, black crystals formed and were isolated (0.18 g, 53% yield). The physical and chemical properties of this compound were identical with those of $(Ph_4P)_2[Fe_4S_4(SPh)_2Cl_2]$ as obtained by the previous procedure.

Bis(tetraphenylphosphonium) Tetrachlorotetra-μ_3-sulfido-tetraferrate(II,III), $(Ph_4P)_2[Fe_4S_4Cl_4]$. (A) In CH_3CN from a 1:8 $[Fe_4(SPh)_6Cl_4]^{2-}$/BzSSSBz Molar Ratio. An amount of 0.38 g (0.23 mmol) of $(Ph_4P)_2[Fe_4(SPh)_6Cl_4]$ was dissolved in 40 mL of CH_3CN. To this solution was added a solution of 0.51 g (1.83 mmol) of BzSSSBz in 10 mL of CH_3CN with stirring. After being stirred 15 min, the solution was filtered and diethyl ether was added to incipient crystallization. When the solution was left to stand for ca. 5 h, crystals formed which were isolated, washed twice with diethyl ether, and dried (0.191 g, 73% yield). The compound was recrystallized from DMF/ether mixtures and was identical with $(Ph_4P)_2(Fe_4S_4Cl_4)$ obtained by the previous procedure and with "authentic"[18] $(Ph_4P)_2(Fe_4S_4Cl_4)$.

(B) From $(Ph_4P)_2[Fe_4S_4(SPh)_2Cl_2]$ and Benzoyl Chloride, PhCOCl. To a solution of 0.35 g (0.26 mmol) of $(Ph_4P)_2[Fe_4S_4(SPh)_2Cl_2]$ in 40 mL of DMF was added a solution of 0.04 mL (0.5 mmol) of PhCOCl in 10 mL of DMF with stirring. The resulting solution was filtered, and to the filtrate was added ether to incipient crystallization. When the mixture was left to stand, dark purple crystals formed and were isolated (0.27 g, 87% yield).

Anal. Calcd for $Fe_4S_4Cl_4C_{48}H_{40}P_2$: C, 49.14; H, 3.41; Fe, 19.11; S, 10.90; Cl, 12.11. Found: C, 49.09; H, 3.60; Fe, 18.81; S, 11.19; Cl, 11.99.

X-ray powder pattern spacings (Å): 11.30 (s), 10.40 (s), 8.70 (s), 7.65 (s), 6.85 (vs), 5.15 (w), 4.40 (m), 4.25 (w).

Bis(tetraphenylphosphonium) Tetrakis(thiophenolato)tetra-μ_3-sulfido-tetraferrate(II,III), $(Ph_4P)_2[Fe_4S_4(SPh)_4]$. An amount of $(Ph_4P)_2[Fe_4S_4(SPh)_2Cl_2]$ (0.24 g, 0.18 mmol) was dissolved in 40 mL of DMF. To this solution was added 0.06 g of KSPh (0.4 mmol), and the mixture was stirred for ca. 10 min. Following filtration ether was added to incipient crystallization, and the filtrate was left to stand for 2 h. Black crystals of $(Ph_4P)_2[Fe_4S_4(SPh)_4]$ formed and were isolated (0.186 g, 70% yield). The visible spectra, NMR spectra, and X-ray powder pattern of this compound were identical with those of "authentic"[19] $(Ph_4P)_2[Fe_4S_4(SPh)_4]$.

X-ray powder pattern spacings (Å): 12.70 (s), 11.00 (s), 8.10 (vs), 7.90 (w), 5.40 (vw), 4.90 (s), 4.50 (w), 3.95 (m), 3.18 (w).

X-ray Diffraction Measurements. Collection and Reduction of Data. Details concerning crystal characteristics and X-ray diffraction methodology are shown in Table I.

Intensity data were obtained on a Picker-Nuclear four-circle diffractometer equipped with a scintillation counter and pulse-height analyzer and automated by a DEC PDP8 computer. Graphite-monochromatized Mo Kα radiation ($2\theta_m = 12.50°$) was used for data collection and cell dimension measurements (Kα_1, $\lambda = 0.709\,26$ Å^{-1}). Intensity data were collected by using a θ–2θ step scan technique.[20] The basic scan step of 0.10° 2θ was adjusted with the angle to allow for α_1–α_2 separation at higher angles. Background measurements, 4 s at each end, were made at ±10 steps from the peak maximum. Three standard reflections were measured every 60 data measurements to monitor crystal quality. No crystal decay was observed.

The raw data were reduced to net intensities, estimated standard deviations were calculated on the basis of counting statistics, Lorentz–polarization corrections were applied, and equivalent reflections were averaged. The estimated standard deviation of the structure factor was taken as the larger of that derived from counting statistics and that derived from the scatter of multiple measurements.

Table I. Summary of Crystal Data, Intensity Collection, and Structure Refinement Data for $(Ph_4P)_2[Fe_4(SPh)_6Cl_4]\cdot 0.75CH_2Cl_2$

formula	$Fe_4S_6Cl_4P_2C_{48}H_{40}\cdot C_{0.75}H_{1.5}Cl_{1.5}$
mol wt	1761.75
a, Å	23.122 (6)
b, Å	13.986 (1)
c, Å	14.189 (4)
α, deg	73.65 (1)
β, deg	80.58 (1)
γ, deg	84.91 (1)
Z	2
d_{calcd}, g/cm^3	1.35
d_{obsd},[a] g/cm^3	1.39 (2)
space group	$P\bar{1}$
cryst dimens, mm	(100) 0.092; (010) 0.71; (102) 0.74
abs coeff μ, cm^{-1}	10.2 (max abs corr 1.74; min 1.10)
radiation	Mo ($\lambda K\alpha_1 = 0.709\,26$)
data collected	2θ: 3–40°; $\pm h, \pm k, \pm l$
unique data	8420
data used in refinement, $F_o^2 > 3\sigma(F_o^2)$	5514
no. of atoms in asymmetric unit	190
no. of variables	661
error in observn of unit weight	2.4
R, %	7.4
R_w, %	10.8

[a] By flotation in a CCl_4/pentane mixture.

The least-squares program used minimizes $\sum w(\Delta|F|)^2$. The weighting function used throughout the refinement of the structure gives zero weight to those reflections with $F^2 \leq 3\sigma(F^2)$ and $w = 1/\sigma^2(F)$ to all others [$\sigma^2(F^2) = (0.06F^2)^2 + \sigma^2(F^2)$ (from counting statistics)].[21]

The scattering factors of the neutral nonhydrogen atoms were taken from the tables of Doyle and Turner,[22] and real and imaginary dispersion corrections[23] were applied to all of them. The spherical hydrogen scattering factors tables of Stewart, Davidson, and Simpson[24] were used. Absorption corrections were applied by using the analytical program ABSORB[25] which uses the analytical method of de Meulenaer and Tompa.[26]

$(Ph_4P)_2[Fe_4(SPh)_6Cl_4]\cdot 0.75CH_2Cl_2$. Crystals suitable for X-ray diffraction work were obtained in a N_2 atmosphere by the slow diffusion of *n*-hexane into a solution of $(Ph_4P)_2[Fe_4(SPh)_6Cl_4]$ in CH_2Cl_2. A fresh crystal was lodged into a quartz capillary tube in an inert atmosphere, and the capillary was sealed. This crystal was used for cell dimension measurements and data collection. The cell dimensions (Table I) were obtained by least-squares refinement on the 2θ values of 13 carefully centered reflections with 2θ between 34° and 45°. A total of 17000 data were collected for a full sphere of reciprocal space. At $2\theta > 40°$ few intensities were "observed", and data collection was terminated.

Determination of the Structure of $(Ph_4P)_2[Fe_4(SPh)_6Cl_4]\cdot 0.75CH_2Cl_2$. A three-dimensional Patterson synthesis map was used to verify the correctness of the atomic positions for the four iron atoms, the six sulfur atoms, and the four chlorine atoms obtained by direct methods using the program MULTAN.[27] The two phosphorus atoms and the 14 phenyl ring carbon atoms were located on subsequent Fourier syntheses following least-squares refinements of the input atomic coordinates. The refinement of all atoms in the anion with isotropic temperature factors in the space group $P\bar{1}$ gave a conventional *R* value of 0.13. Further refinement of the structure with anisotropic temperature factors for the noncarbon heavy atoms and for the carbon atoms of the phenyl rings in the anion

---

(19) Que, L., Jr.; Bobrik, M. A.; Ibers, J. A.; Holm, R. H.; *J. Am. Chem. Soc.* **1974**, *96*, 4168.

(20) Baenziger, N. C.; Foster, B. A.; Howells, M.; Hcwells, R.; Vander Valk, P.; Burton, D. J. *Acta Crystallogr., Sect. B* **1977**, *B33*, 2327.

(21) Grant, D. F.; Killean, R. C. G.; Lawrence, J. L. *Acta Crystallogr., Sect. B* **1969**, *B25*, 374.

(22) Doyle, P. A.; Turner, P. S. *Acta Crystallogr., Sect. A* **1968**, *A24*, 390.

(23) Cromer, D. T.; Liberman, D. *J. Chem. Phys.*, **1970**, *53*, 1891.

(24) Stewart, R. F.; Davidson, E. R.; Simpson, W. T. *J. Chem. Phys.* **1965**, *42*, 3175.

(25) Templeton, L.; Templeton, D. "ABSORB"; American Crystallographers Association Meeting: Storrs, CT, Abstract E10, p 143; modified for local use by F. J. Hollander.

(26) deMeulenaer, J.; Tompa, H. *Acta Crystallogr.* **1965**, *19*, 1014.

(27) Main, P.; Woolfson, M. M.; Germain, G. "MULTAN, A Computer Program for the Automatic Solution of Crystal Structures"; University of York: York, England 1971.

Table II. Positional and Thermal Parameters for the Noncarbon Atoms[a] and the Carbon Atoms[b] Attached to the Thiolate Sulfur Atoms in $[(C_6H_5)_4P]_2[Fe_4(SC_6H_5)_6Cl_4]$

atom	x	y	z	atom	x	y	z
Fe(1)	0.27074 (8)	0.1961 (1)	−0.0358 (1)	S(3)	0.3084 (1)	0.0740 (2)	0.0917 (2)
Fe(2)	0.12780 (6)	0.2379 (1)	0.1492 (1)	S(4)	0.1593 (1)	0.1064 (2)	0.2791 (2)
Fe(3)	0.26967 (7)	0.3704 (1)	0.1385 (1)	S(5)	0.3001 (1)	0.2253 (2)	0.2562 (2)
Fe(4)	0.26288 (7)	0.0751 (1)	0.2521 (1)	S(6)	0.1654 (1)	0.3774 (2)	0.1794 (2)
Cl(1)	0.3071 (2)	0.1620 (3)	−0.1807 (2)	C(1)S(1)	0.1364 (5)	0.1445 (9)	−0.0536 (9)
Cl(2)	0.3135 (1)	0.5059 (2)	0.1451 (2)	C(1)S(2)	0.2840 (5)	0.4441 (9)	−0.1163 (8)
Cl(3)	0.0293 (1)	0.2579 (2)	0.1692 (2)	C(1)S(3)	0.2965 (6)	−0.0467 (8)	0.0748 (8)
Cl(4)	0.2942 (2)	−0.0609 (2)	0.3636 (3)	C(1)S(4)	0.1246 (5)	0.0012 (8)	0.2703 (8)
S(1)	0.1689 (1)	0.2320 (2)	−0.0124 (2)	C(1)S(5)	0.2821 (5)	0.2431 (8)	0.3791 (8)
S(2)	0.3054 (1)	0.3415 (2)	−0.0172 (2)	C(1)S(6)	0.1398 (5)	0.4918 (8)	0.0968 (8)

atom	B_{11}	B_{22}	B_{33}	B_{12}	B_{13}	B_{23}
Fe(1)	5.3 (1)	2.94 (8)	3.25 (8)	−0.20 (7)	−0.16 (6)	−0.80 (6)
Fe(2)	3.16 (8)	3.22 (8)	3.02 (7)	0.22 (6)	−0.56 (5)	−0.93 (6)
Fe(3)	3.35 (8)	3.01 (8)	3.38 (7)	0.02 (6)	−0.87 (6)	−0.87 (6)
Fe(4)	4.53 (9)	2.89 (8)	3.99 (8)	0.51 (7)	−1.79 (6)	−0.82 (6)
Cl(1)	9.4 (2)	5.7 (2)	4.4 (2)	−0.1 (2)	0.6 (1)	−2.0 (1)
Cl(2)	5.2 (2)	3.2 (1)	5.8 (2)	−0.3 (1)	−1.6 (1)	−1.3 (1)
Cl(3)	3.4 (1)	5.6 (2)	5.4 (2)	0.1 (1)	−0.8 (1)	−1.1 (1)
Cl(4)	10.0 (3)	3.7 (2)	6.1 (2)	1.4 (2)	−4.1 (2)	−0.6 (1)
S(1)	4.7 (2)	3.9 (1)	3.8 (1)	0.4 (1)	−0.7 (1)	−1.3 (7)
S(2)	4.5 (2)	3.5 (1)	3.6 (1)	−0.3 (1)	−0.2 (1)	−0.7 (1)
S(3)	5.5 (2)	3.3 (1)	4.6 (1)	0.4 (1)	−0.7 (1)	−1.3 (1)
S(4)	4.6 (2)	3.5 (1)	3.3 (1)	−0.1 (1)	−0.8 (1)	−0.5 (1)
S(5)	4.6 (2)	3.4 (1)	4.0 (1)	0.3 (1)	−1.6 (1)	−1.0 (1)
S(6)	3.7 (1)	3.3 (1)	3.6 (1)	0.3 (1)	−0.9 (1)	−1.0 (1)
C(1)S(1)	4.1 (6)	5.0 (7)	4.7 (7)	0.5 (6)	−2.2 (5)	−1.6 (5)
C(1)S(2)	4.8 (6)	3.1 (6)	3.4 (6)	−0.6 (5)	−0.2 (5)	−0.2 (4)
C(1)S(3)	5.6 (7)	3.2 (6)	3.2 (6)	0.3 (6)	−0.1 (5)	−1.1 (5)
C(1)S(4)	4.6 (7)	3.7 (6)	3.5 (5)	−0.3 (5)	−0.9 (5)	−0.6 (4)
C(1)S(5)	3.7 (6)	3.7 (6)	3.1 (6)	0.1 (5)	−1.5 (4)	−1.2 (5)
C(1)S(6)	2.9 (5)	1.6 (5)	4.2 (6)	0.2 (4)	0.3 (4)	0.0 (4)

[a] The thermal parameters are in units of Å². The temperature factor has the form $T = -\Sigma(^1/_4 B_{ij}H_iH_ja_i{}^*a_j{}^*)$ where H is the Miller index, a* is the reciprocal cell length and i and j are cycled 1–3. [b] The temperature factor has the form $T = -B[((\sin\theta)/\lambda)^2]$. B in Å².

gave a conventional R value of 0.095.

At this stage a difference Fourier synthesis map revealed the presence of CH_2Cl_2 solvent at locations around $x = 0.46$, $y = 0.27$, $z = 0.80$ and $x = 0.47$, $y = 0.12$, $z = 0.16$. Because of the small fractional occupancy of the CH_2Cl_2 solvent molecules at these sites (0.40 for one and 0.35 for the other), the CH_2Cl_2 molecules were refined as rigid groups[28] with an overall temperature factor for each group. Refinement converged to a conventional R value of 0.083. In the final refinement the 70 hydrogen atoms were included in the structure factor calculation at their calculated positions (0.95 Å from the C atoms) but were not refined. The final R value was 0.074; the weighted R (Table I) was 0.108. During the last cycle of refinement all parameters shifts were less than 10% of their esd. The final parameters of the structure with their estimated standard deviations as calculated from the inverse least-squares matrix are given in Table II.

Crystallographic Results. The final atomic positional and thermal parameters with standard deviations derived as described previously are compiled in Table II. Intramolecular distances and angles are given in Table III, and a comparison between various $M_4(SPh)_6$ "adamantane" cores is presented in Table IV.

The atom labeling scheme is shown in Figure 1. A stereopair drawing of the $[Fe_4(SC_6H_5)_6Cl_4]^{2-}$ anion is shown in Figure 2, and a stereopair drawing of the unit cell contents is shown in Figure 3.

Deposited with the microfilm version of the journal are (a) tables of the observed values of F, their esd's, and the $|F_o| - |F_c|$ values (b) the final atomic positional and thermal parameters for the phosphorus and carbon atoms of the cations, of the carbon atoms of the anion (excluding the C atoms bound to sulfur), and of all the hydrogen atoms, and (c) a table of weighted least-squares planes and dihedral angles.

Results and Discussion

Synthesis of the $[Fe_4(SPh)_6X_4]^{2-}$ Clusters (X = Cl, Br). Of particular relevance to the synthetic aspects of this work are the synthetic and crystallographic studies of Dance and Calabrese, who isolated the first $[M_4(SPh)_{10-x}Cl_x]^{2-}$ complexes (M = Co(II), $x = 0$;[9] Co(II), $x = 2$;[9] Zn(II), $x = 0$;[9,11] Zn(II), $x = 2$[9,11]) and structurally characterized the $[Co_4(SPh)_{10}]^{2-}$[9b] and $[Zn_4(SPh)_8Cl_2]^{2-}$[11] clusters.

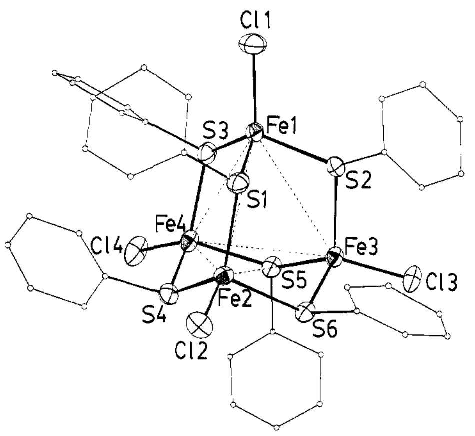

Figure 1. Structure and labeling of the $[Fe_4(SC_6H_5)_6Cl_4]^{2-}$ anion. Thermal ellipsoids as drawn by ORTEP (Johnson, C. K. ORNL-3794; Oak Ridge National Laboratory: Oak Ridge, TN, 1965) represent the 50% probability surfaces. Carbon atoms are drawn artificially small.

More recently the synthesis and structural characterization of the $[Fe_4(SPh)_{10}]^{2-}$ cluster also was reported.[10] The $[Fe_4(SPh)_6X_4]^{2-}$ complexes unambiguously characterized in this paper represent the first structurally characterized examples of the $[M_4(SPh)_6X_4]^{2-}$ clusters with terminal halide and only doubly bridging thiophenolate ligands.

The formation of the $(R_4N)_2[Fe_4(SPh)_{10}]^{2-}$ cluster has been reported[10,16] to occur in methanol solution from $FeCl_2 \cdot 2H_2O$, NaSPh, and R_4NCl in a 1:3:0.5 molar ratio. In our studies of the solution chemistry of the $[Fe(SPh)_4]^{2-}$ dianion, we have obtained also salts of the $[Fe_4(SPh)_{10}]^{2-}$ cluster in essentially similar reactions. The isolation and structural characteriziation of

---

[28] Scheringer, C. *Acta Crystallogr.* **1963**, *16*, 546. The CH_2Cl_2 molecules were fixed with C–H = 0.95 Å, C–Cl = 1.772 Å, Cl–C–Cl = 111.8°, and H–C–H = 112°.

Table III. Selected Interatomic Distances (Å) and Angles (Deg) in $[Fe_4(SC_6H_5)_6Cl_4]^{2-}$

Distances

Fe(1)-Fe(2)	3.980 (2)	Fe(1)-Cl(1)	2.252 (4)
Fe(1)-Fe(3)	3.928 (2)	Fe(2)-Cl(2)	2.252 (3)
Fe(1)-Fe(4)	3.939 (2)	Fe(3)-Cl(3)	2.257 (3)
Fe(2)-Fe(3)	3.870 (2)	Fe(4)-Cl(3)	2.254 (3)
Fe(2)-Fe(4)	3.928 (2)	mean^a	2.254 (3)
Fe(3)-Fe(4)	3.996 (2)	S(1)-S(3)	3.990 (4)
mean^a	3.94 (4)	S(2)-S(6)	4.007 (4)
Fe(1)-S(1)	2.352 (4)	S(1)-S(4)	3.991 (4)
Fe(1)-S(2)	2.347 (3)	S(3)-S(4)	4.070 (4)
Fe(1)-S(3)	2.337 (3)	mean^{a,b}	4.01 (4)
Fe(2)-S(1)	2.356 (3)	S(1)-S(2)	3.611 (4)
Fe(2)-S(4)	2.368 (3)	S(2)-S(3)	3.622 (4)
Fe(2)-S(6)	2.374 (3)	S(2)-S(5)	3.746 (4)
Fe(3)-S(2)	2.361 (3)	S(5)-S(6)	3.746 (4)
Fe(3)-S(5)	2.371 (3)	S(4)-S(6)	3.660 (4)
Fe(3)-S(6)	2.385 (3)	S(1)-S(6)	3.816 (4)
Fe(4)-S(3)	2.350 (4)	S(3)-S(5)	3.539 (4)
Fe(4)-S(5)	2.358 (3)	S(4)-S(5)	3.712 (4)
Fe(4)-S(4)	2.383 (3)	mean^a	3.68 (9)
mean^a	2.362 (15)	S(1)-C(1)S(1)	1.764 (13)
S(1)-Cl(1)	3.889 (5)	S(2)-C(1)S(2)	1.802 (11)
S(2)-Cl(1)	3.863 (5)	S(3)-C(1)S(3)	1.822 (12)
S(3)-Cl(1)	3.715 (4)	S(4)-C(1)S(4)	1.782 (12)
S(1)-Cl(2)	3.846 (4)	S(5)-C(1)S(5)	1.807 (11)
S(4)-Cl(2)	3.810 (4)	S(6)-C(1)S(6)	1.813 (10)
S(6)-Cl(2)	3.734 (4)	mean^a	1.80 (2)
S(2)-Cl(3)	3.717 (4)		
S(5)-Cl(3)	3.815 (4)		
S(6)-Cl(3)	3.904 (4)		
S(3)-Cl(4)	3.762 (4)		
S(4)-Cl(4)	3.870 (4)		
S(5)-Cl(4)	3.869 (4)		
mean^a	3.82 (7)		

Angles

Fe(2)-Fe(1)-Fe(3)	58.59 (4)	S(1)-Fe(1)-S(3)	116.64 (15)
Fe(2)-Fe(1)-Fe(4)	59.47 (4)	S(1)-Fe(2)-S(4)	115.30 (14)
Fe(3)-Fe(1)-Fe(4)	61.05 (4)	S(2)-Fe(3)-S(6)	115.18 (14)
Fe(1)-Fe(2)-Fe(3)	60.03 (4)	S(3)-Fe(4)-S(4)	118.59 (15)
Fe(1)-Fe(2)-Fe(4)	59.73 (4)	mean^{a,b}	116.4 (2)
Fe(3)-Fe(2)-Fe(4)	61.64 (4)	S(1)-Fe(1)-S(2)	100.41 (13)
Fe(1)-Fe(3)-Fe(2)	61.38 (4)	S(2)-Fe(1)-S(3)	101.29 (14)
Fe(1)-Fe(3)-Fe(4)	59.60 (4)	S(1)-Fe(2)-S(6)	107.56 (14)
Fe(2)-Fe(3)-Fe(4)	59.89 (4)	S(4)-Fe(2)-S(6)	101.04 (13)
Fe(1)-Fe(4)-Fe(2)	60.79 (4)	S(2)-Fe(3)-S(5)	104.66 (14)
Fe(1)-Fe(4)-Fe(3)	59.35 (4)	S(6)-Fe(3)-S(5)	103.91 (13)
Fe(2)-Fe(4)-Fe(3)	58.46 (4)	S(3)-Fe(4)-S(5)	97.44 (14)
mean^a	60 (1)	S(4)-Fe(4)-S(5)	103.03 (13)
Fe(1)-S(1)-C(1)S(1)	106.4 (4)	mean^a	102.4 (3)
Fe(2)-S(1)-C(1)S(1)	113.0 (5)	Fe(1)-S(1)-Fe(2)	115.4 (1)
Fe(2)-S(4)-C(1)S(4)	103.3 (3)	Fe(1)-S(2)-Fe(3)	113.1 (1)
Fe(4)-S(4)-C(1)S(4)	108.4 (4)	Fe(1)-S(3)-Fe(4)	114.3 (1)
Fe(1)-S(3)-C(1)S(3)	107.2 (4)	Fe(2)-S(4)-Fe(4)	111.5 (1)
Fe(4)-S(3)-C(1)S(3)	107.2 (4)	Fe(3)-S(5)-Fe(4)	115.3 (1)
Fe(1)-S(2)-C(1)S(2)	107.3 (4)	Fe(2)-S(6)-Fe(3)	108.8 (1)
Fe(3)-S(2)-C(1)S(2)	110.6 (4)	mean^a	113 (2)
Fe(2)-S(6)-C(1)S(6)	109.9 (4)		
Fe(3)-S(6)-C(1)S(6)	106.0 (3)		
Fe(3)-S(5)-C(1)S(5)	109.3 (3)		
Fe(4)-S(5)-C(1)S(5)	110.4 (4)		
mean^a	108.3 (25)		
Cl(1)-Fe(1)-S(1)	115.3 (2)		
Cl(1)-Fe(1)-S(2)	114.2 (2)		
Cl(1)-Fe(1)-S(3)	108.1 (2)		
Cl(2)-Fe(2)-S(1)	113.2 (2)		
Cl(2)-Fe(2)-S(4)	111.1 (1)		
Cl(2)-Fe(2)-S(6)	107.6 (2)		
Cl(3)-Fe(3)-S(2)	107.2 (2)		
Cl(3)-Fe(3)-S(5)	111.0 (1)		
Cl(3)-Fe(3)-S(6)	114.5 (2)		
Cl(4)-Fe(4)-S(3)	109.6 (2)		
Cl(4)-Fe(4)-S(4)	113.1 (2)		
Cl(4)-Fe(4)-S(5)	114.0 (2)		
mean	112 (3)		
mean value of all L-Fe-L angles	109.3 (5.9)		

[a] Estimated standard deviation calculated from scatter of values around mean $s \simeq \sigma = [\Sigma_i(\chi_i^2 - n\bar{\chi}^2)/(n-1)]^{1/2}$. [b] S_i-S_j distances and S_i-Fe-S_j angles affected by the axial-axial disposition of the $S_{i,j}$-C_6H_5 bonds in the Fe_3S_3 "chair" components of the Fe_4S_6 adamantane cage (see text). [c] The C-C bond distances in the 14 phenyl rings span the range from 1.22 (3) to 1.55 (3) Å with a mean value of 1.38 Å and a standard deviation from the mean (as described in footnote *a*) (above) of 0.05 Å.

Table IV. A Comparison of the M_4S_6 "Adamantane" Cores in the $[M_4(SPh)_x(Cl)_y]^{2-}$ Complexes

	complexes				
	$[Fe_4(SPh)_6Cl_4]^{2-a}$	$[Fe_4(SPh)_{10}]^{2-c}$	$[Co_4(SPh)_{10}]^{2-d}$	$[Zn_4(SPh)_8Cl_2]^{2-e}$	$[Cu_4(SPh)_6]^{2-f}$
$\overline{M\text{-}M}$,^{b} Å	3.94 (4)	3.93 (5)	3.87 (2)	3.90 (5)	2.76 (2)^c 2.76 (4)^d
$\overline{M\text{-}S_b}$, Å	2.362 (15)	2.365 (17)	2.322 (11)	2.358 (15)	2.29 (3)^c 2.29 (1)^d
$\overline{M\text{-}S_t}$, Å	...	2.287 (15)	2.258 (4)	2.266 (13)	...
$\overline{M\text{-}Cl_t}$, Å	2.254 (3)	...	...	2.248 (10)	...
$\overline{S_b\text{-}S_b}$, Å	3.79 (18)		3.74 (14)	3.81 (12)	3.94 (20)^c 3.94 (6)^d
S-C_α, Å	1.80 (2)		1.78 (1)	1.74 (7)	
$\overline{S_b\text{-}M\text{-}S_b}$, deg	107 (7)		107 (6)	108 (5)	120 (10)^c
$\overline{M\text{-}S_b\text{-}M}$, deg	113 (2)		113 (1)	112 (2)	73.8 (10)^c 74.3 (12)^d

[a] This work. [b] $s \simeq \sigma = [\Sigma_i(\chi_i^2 - n\bar{\chi}^2)/(n-1)]^{1/2}$. [c] Reference 10. [d] Reference 9b. [e] Reference 11. [f] References 12 and 13.

$[Fe_4(SPh)_{10}]^{2-}$ and the apparently concurrent investigation of the solution chemistry of the cluster by Holm and co-workers[10] prompted us to redirect our studies in the syntheses and reactions of the $[Fe_4(SPh)_xCl_{10-x}]^{2-}$ clusters.

We have observed that in mixtures, where the PhS^- to Fe(II) ratio is >2.5 and the Cl^- to Fe(II) ratio is <1, the novel $[Fe_4(SPh)_{10}]^{2-}$ cluster[10] is present as the predominant species and can be isolated in good yields. When the PhS^- to Fe(II) ratio becomes >4.0, the known[7,8] $[Fe(SPh)_4]^{2-}$ anion forms. In mixtures, where the PhS^- to Fe(II) ratio is <2 and the X^- to Fe(II) ratio is >1 ($X = Cl^-, Br^-$), the predominant species in solution are the $[Fe_4(SPh)_6X_4]^{2-}$ clusters. These anions can be isolated as the

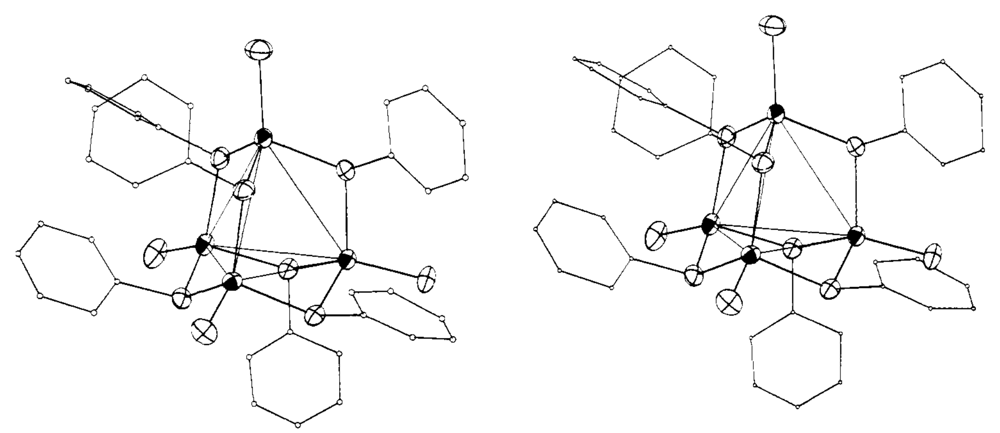

Figure 2. Stereoscopic view of $[Fe_4(SC_6H_5)_6Cl_4]^{2-}$ as drawn by ORTEP.

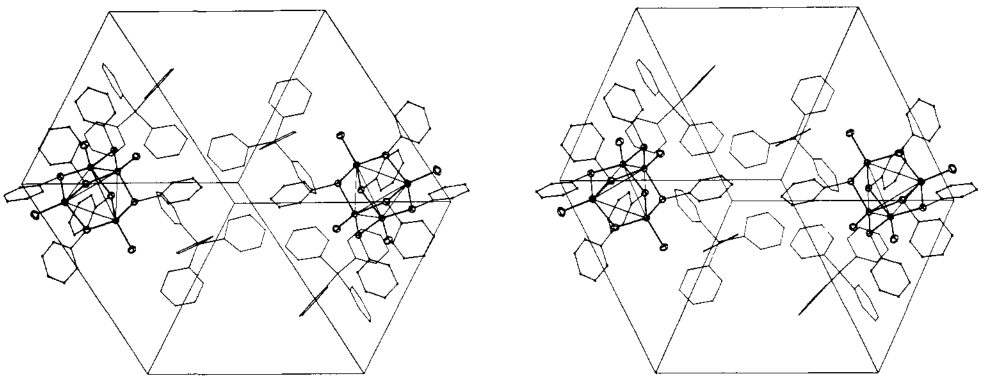

Figure 3. Unit cell contents of $[(C_6H_5)_4P]_2[Fe_4(SC_6H_5)_6Cl_4]\cdot 0.75CH_2Cl_2$. The CH_2Cl_2 molecules are not included in the figure.

Ph_4P^+ salts, in excellent yields, either in the reaction of $(Ph_4P)_2[Fe(SPh)_4]$ with $FeCl_2$ in a 1:2.4 molar ratio or in the reaction of $FeCl_2$, Ph_4PCl, and KSPh in a 2:1:3 molar ratio. The formation of mixed halo thiophenolato, $[Fe_4(SPh)_x(X)_{10-x}]^{2-}$, clusters in Fe(II), PhS^-, and Cl^- mixtures has a precedent in analogous Co(II) and Zn(II) PhS^-/Cl^- systems.[9b,11] For the $Co(II)/PhS^-/Cl^-$ system a series of equilibria have been observed in solution[9b] and involve such species as $[Co_4(SPh)_{10}]^{2-}$, $[Co_4(SPh)_6Cl_4]^{2-}$, $[Co(SPh)_4]^{2-}$, $[Co_4(SPh)_8Cl_2]^{2-}$, and $[Co_2(SPh)_6]^{2-}$. Similar complex equilibria of analogous complexes very likely occur in the $Fe(II)/PhS^-/Cl^-$ system as well.

The isotropically shifted proton NMR spectra of $[Fe_4(SPh)_6Cl_4]^{2-}$ and of the corresponding p-CH_3 derivative are shown in Figure 4 and are tabulated in Table V. As expected only bridging phenyl or p-tolyl groups are present in these anions with isotropically shifted o-H, m-H, and p-H (CH_3) resonances very similar in position to the corresponding resonances of the bridging SPh ligands in $[Fe_4(SPh)_{10}]^{2-}$.[16] The low-energy electronic absorption expected for the $10Dq$ transition of the tetrahedral $ClFe^{II}(SPh)_3$ subunits in $[Fe_4(SPh)_6Cl_4]^{2-}$ in CH_3CN solution occurs at 1800 nm with ϵ 370.

The Crystal and Molecular Structure of $(Ph_4P)_2[Fe_4(SPh)_6Cl_4]$. Determination of the crystal structure shows a lattice with the individual $[Fe_4(SPh)_6Cl_4]^{2-}$ anions well separated from each other by the $P(C_6H_5)_4{}^+$ counterions. The anionic cluster contains the four iron atoms located at the vertices of a nearly regular tetrahedron with the six benzenethiolate ligands bridging along the edges of the tetrahedron. The four chloride ligands bound terminally one on each iron atom complete the coordination for each of the four tetrahedrally coordinated iron atoms in the $[(\mu\text{-}SPh)_6(FeCl)_4]^{2-}$ cluster (Figures 1 and 2). The *entire* cluster does not possess crystallographically imposed symmetry or any approximate symmetry. The $Fe_4S_6Cl_4$ core however approaches an ideal T_d point-group symmetry with the four iron atoms arranged at the vertices of an inner tetrahedron, the six bridging sulfur atoms at the vertices of an approximate octahedron and the four chlorine atoms at the vertices of an outer tetrahedron.

Table V. Isotropic Shifts[a] of the Proton Resonances[b] in the $[Fe_4(SPh)_6X_4]^{2-}$ Complexes (CD_3CN Solutions at ~27 °C)

	$\Delta H/H_0$, ppm			
complex	o-H	m-H	p-H, -CH_3	ref
$[Fe_4(SPh)_6Cl_4]^{2-}$	+27.62	−7.2	+24.6	*c*
$[Fe_4(S\text{-}p\text{-}tol)_6Cl_4]^{2-}$	+27.64	−7.2	−20.95	*c*
$[Fe_4(SPh)_6Br_4]^{2-}$	+24.2 (b)	−8.8 (b)	+23.7 (b)	*c*
$[Fe_4(SPh)_{10}]^{2-}$	+10.4 (t)	−9.00 (t)	+16.2 (t)	*d*
	+16.2 (b)	−9.00 (b)	+19.2 (b)	
$[Fe_4(S\text{-}p\text{-}tol)_{10}]^{2-}$	+10.2 (t)	−9.07 (t)	−16.9 (t)	*d*
	+16.4 (b)	−8.88 (b)	−19.3 (b)	

[a] $(\Delta H/H_0)_{iso} = (\Delta H/H_0)_{obsd} - (\Delta H/H_0)_{dia}$; diamagnetic shifts are those of the free thiols. [b] b = bridging, t = terminal. [c] This work. [d] Reference 16 (resonances observed in CD_3CN solutions at ~27 °C).

Distortions from the ideal T_d symmetry for this arrangement are apparent in the slightly unequal distances in each of the Fe–Fe, S–S, and Cl–Cl groups of intracore dimensions (Table III) and from deviations of the internal S_b–Fe–S_b and Fe–S_b–Fe angles from 109.5%.

The distortions from ideal T_d symmetry in the Fe_4S_6 adamantane cage are apparent in the dihedral angles of selected planes. The mean value of the dihedral angles between the adjacent trigonal faces of the S_6 octahedron at 70.6° (3.4°) is very close to the theoretical value of 70.52°. Similarly the dihedral angles between the S_4 planes perpendicular to the fourfold axes of the S_6 octahedron (S(1)S(3)S(5)S(6), S(1)S(2)S(4)S(5), S(2)S(3)S(4)S(6); Figure 1) are within the range 96.12–86.75° with a mean value of 92 ± 5°. The appropriate dihedral angles between the six σ_d planes ($Fe_iFe_jS_kS$) in the Fe_4S_6 cage, which also are expected to be 90°, are within the range 87.52–91.15° with a mean value of 89 ± 2°.

Selected interatomic distances and angles are presented in Table III. An examination of the individual S_3FeCl tetrahedral units in the $[Fe_4(SPh)_6Cl_4]^{2-}$ anion shows that one of the S–Fe–S angles

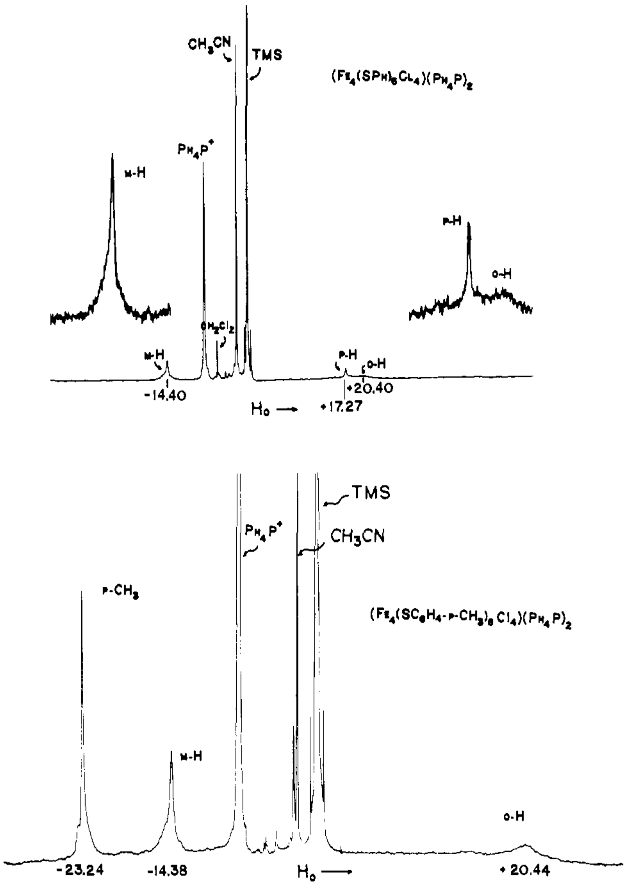

Figure 4. ^{1}H NMR spectra (100 MHz) of $(Ph_4P)_2[Fe_4(SPh)_6Cl_4\cdot 0.75CH_2Cl_2]$ and $(Ph_4P)_2[Fe_4(SC_6H_4\text{-}p\text{-}CH_3)_6Cl_4]$ in CD_3CN at ~27 °C. Inserts represent expanded versions of the spectra.

in each unit is considerably larger than 109.5°, while the other two are considerably smaller than 109.5°. The large S_b–Fe–S_b angles involve sulfur atoms on which the phenyl rings (and the S–C_α vectors) are directed axially with respect to the $Fe_3(S_b)_3$ chairs of the adamantane core. Thus in the Fe(1)S(1)Fe(2)S(4)Fe(4)S(3) chair (Figure 1 and 2), where all three of the S–C_α vectors are axially directed, the S(1)–Fe(1)–S(3), S(1)–Fe(2)–S(4), and S(3)–Fe(4)–S(4) angles are 116.64°, 115.30°, and 118.59°, respectively (Table III). There is only one other chair in the adamantane "cage" that contains two axially disposed S–C_α vectors. In this chair, Fe(1)S(2)Fe(3)S(6)Fe(2)S(1), the axial vectors are S(2)–C_α and S(6)–C_α and the S(2)–Fe(3)–S(6) angle is 115.18°. These enlarged angles, which very likely arise because of repulsions between the phenyl rings, force the remaining S_{ax}–Fe–S_{eq} and S_{eq}–Fe–S_{eq} angles to become smaller than 109.5° (Table III). As expected, the smaller angles in this group are the S_{eq}–Fe–S_{eq} angles S(3)–Fe(4)–S(5), S(2)–Fe(3)–S(5), S(3)–Fe(1)–S(2), and S(6)–Fe(2)–S(4) at 97.44, 104.66°, 101.29, and 101.04°, respectively. These differences between S_{ax}–M–S_{ax}, S_{ax}–M–S_{eq}, and S_{eq}–M–S_{eq} angles have been noted also in the structure of the $(Zn_4(SPh)_8Cl_2)^{2-}$ cluster and have been interpreted[11] in terms of possible phenyl ring repulsions. In the $[Fe_4(SPh)_6Cl_4]^{2-}$, differences in the S_b–Fe–S_b angles are reflected also in the S_b–S_b distances. A group of four long S–S distances are found with the sulfur atoms associated with the S_{ax}–Fe–S_{ax} angles and cause deviations of the six bridging sulfur atom arrangement from idealized octahedral symmetry. The mean value of the S_b–Fe–Cl angles at 112 (3)° indicates that the iron atoms are slightly displaced in the direction of the pseudo threefold axes and away from the center of the cluster. This slight displacement also is apparent in the differences between the $\overline{\text{Fe–Fe}}$ and $\overline{S_b\text{–}S_b}$ distances of 3.94 (4) and 3.79 (18) Å. The $\overline{\text{Fe–Fe}}$ distance to the $\overline{\text{Fe–}S_b}$ distance ratio of 1.668 is greater than the idealized value of 1.633 and very similar to the corresponding ratio reported[9b] for the $[Co_4(SPh)_{10}]^{2-}$ cluster (1.666). For the later cluster the same distortions have been observed and analyzed.[9b] As in the case of $[Co_4(SPh)_{10}]^{2-}$ the elongation of the M–M distances in the present structure as well as their magnitude preclude any significant direct M–M bonding. A comparison of some of the intramolecular distances and angles in $[Fe_4(SPh)_6Cl_4]^{2-}$ to similar parameters in other clusters that contain the central M_4S_6 core are shown in Table IV. The similarity of the Fe_4S_6 core in $[Fe_4(SPh)_6Cl_4]^{2-}$ to the Co_4S_6, Zn_4S_6, and Fe_4S_6 cores in the $[Co_4(SPh)_{10}]^{2-}$,[9b] $[Zn_4(SPh)_8Cl_2]^{2-}$[11], and $[Fe_4(SPh)_{10}]^{2-}$[10] clusters respectively is obvious and small differences in the M–M distances correlate with the tetrahedral (high spin) radii of the divalent ions, Co < Zn < Fe. Other interatomic distances and angles in the M_4S_6 cores of these molecules are similar to within one or two standard deviations from their mean values.

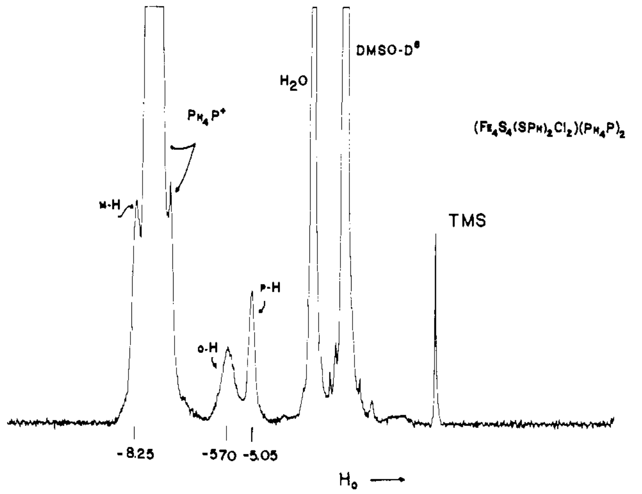

Figure 5. ^{1}H NMR spectrum (100 MHz) of $(Ph_4P)_2[Fe_4S_4(SPh)_2Cl_2]$ in dimethylsulfoxide-d_6 (Me_2SO-d_6) at ~27 °C.

Pronounced differences between the $[M_4(SPh)_6]^{2+}$ cores and the $[Cu_4(SPh)_6]^{2-}$ cluster[12,13] are evident in the corresponding M–M distances and the M–S_b–M angles (Table IV). Thus, larger M–M distances and M–S_b–M angles are found in the $[M_4(SPh)_6]^{2+}$ cores (~3.95 Å and ~112°) by comparison to corresponding values (2.76 Å and 74°) in the $[Cu_4(SPh)_6]^{2-}$ cluster. These differences very likely reflect predominant coulombic M–M repulsions in the former and possibly attractive Cu–Cu interactions in the latter.

The mean value of the Fe(II)–S bond lengths in the present structure, 2.362 (15) Å, is comparable to the value determined[8c] for the $\overline{\text{Fe(II)–S}}$ bond length in the $[Fe(SPh)_4]^{2-}$ complex, 2.353 (9) Å, However, the $\overline{\text{Fe(II)–Cl}}$ bond length (Table III) at 2.254 (3) Å is shorter than the $\overline{\text{Fe–Cl}}$ bond length in $[FeCl_4]^{2-}$ (2.302(18)[29] and 2.292 (2) Å[30]). These observations suggest that slight electronic structure perturbations have occurred in the individual $ClFe(SPh)_3$ units. Evidence for indirect weak electronic coupling between the iron atoms is apparent in the magnetic properties and Mössbauer spectra of $[Fe_4(SPh)_6X_4]^{2-}$, which will be reported in detail in a forthcoming publication.[31]

Reactions of $[Fe_4(SPh)_6Cl_4]^{2-}$. The versatility of dibenzyl trisulfide (BzSSSBz) in its reactions with sulfur complexes (vide infra) prompted us to initiate this study and attempt to explore the reactivity of BzSSSBz toward bridging mercaptido ligands. The $[Fe_4(SPh)_6Cl_4]^{2-}$ cluster reacts readily with BzSSSBz, and

---

(29) Trinh-Toan; Dahl, L. F. *J. Am. Chem. Soc.* **1971**, *93*, 2654.

(30) Lauher, J. W.; Ibers, J. A. *Inorg. Chem.* **1975**, *14*, 348.

(31) Preliminary Mössbauer measurements at 77 K show isomer shifts and quadrupole splittings for the $[Fe_4(SPh)_6Cl_4]^{2-}$ and $[Fe_4(SPh)_6Br_4]^{2-}$ clusters at 0.79, 3.15 mm/s and 0.79, 3.31 mm/s, respectively. The Mössbauer spectrum of $[Fe_4(SPh)_6Cl_4]^{2-}$ shows no splitting in an applied magnetic field of ~7 kG. This observation as well as preliminary magnetic susceptibility measurements suggest that the iron atoms in $[Fe_4(SPh)_6Cl_4]^{2-}$ are antiferromagnetically coupled. (Simopoulos, A.; Petrouleas, V.; Kostikas, A., private communication).

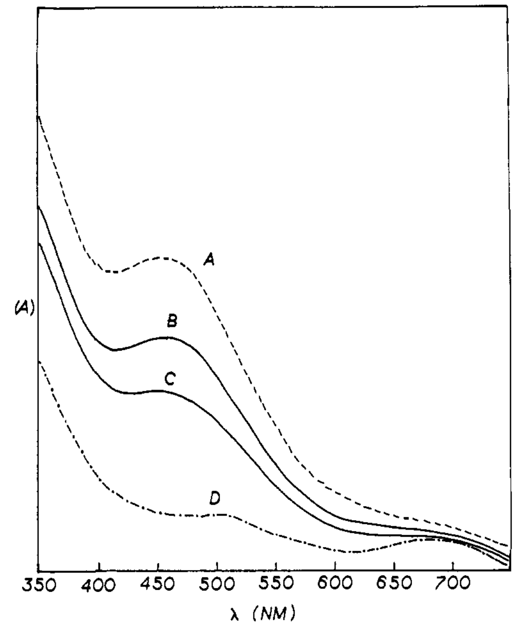

Figure 6. Visible spectra of equimolar dimethylformamide (DMF) solutions of A, $(Ph_4P)_2[Fe_4S_4(SPh)_4]$, B, $(Ph_4P)_2[Fe_4S_4(SPh)_2Cl_2)$, *C*, 1:1 mixture of $(Ph_4P)_2[Fe_4S_4(SPh)_4]$ and $(Ph_4P)_2(Fe_4S_4Cl_4)$, and D, $[Ph_4P]_2(Fe_4S_4Cl_4)$. The total concentration in all cases was 5.83×10^{-4} M.

the nature of the reaction products depends on both the type of the solvent media used and of the stoichiometry.

In reactions, where the BzSSSBz to $[Fe_4(SPh)_6Cl_4]^{2-}$ ratio does not exceed 2, only partial oxidation of the phenyl mercaptides occurs and the major product that is isolated in good yields is the "mixed" chloro thiophenalato cubane, $[Fe_4S_4(SPh)_2Cl_2]^{2-}$, regardless of the solvent used (CH_3CN or a CH_3CN/DMF mixture).

The proton NMR spectrum of $(Ph_4P)_2[Fe_4S_4(SPh)_2Cl_2]$ in CH_3CN solution (Figure 5) resembles the spectrum of $[Fe_4S_4(SPh)_4]^{2-}$.[6] The isotropically shifted resonances for the *o*-H, *m*-H, and *p*-H protons in II are observed at 5.70, 8.25, and 5.05 ppm, respectively. By comparison the analogous resonances in the ^1H NMR spectrum of $[Fe_4S_4(SPh)_4]^{2-}$ occur at 5.88, 8.18, and 5.28 ppm.

The NMR spectra of reaction mixtures containing BzSSSBz and $[Fe_4(SPh)_6Cl_4]^{2-}$ in 1:1, 2:1, 3:1, and 4:1 molar ratios in DMF solution show the resonance attributed to the isotropically shifted *p*-phenyl hydrogen atom of the $[Fe_4S_4(SPh)_2Cl_2]^{2-}$ cluster as the major component in that region of the spectrum. In all instances additional *p*-phenyl hydrogen resonances are observed which very likely arise from other mixed cubanes $[Fe_4S_4(SPh)_x(Cl)_{4-x}]^{2-}$. The isolation of pure crystalline $(Ph_4P)_2[Fe_4S_4(SPh)_2Cl_2]$ from these reaction mixtures is possible because of the relative insolubility of $(Ph_4P)_2[Fe_4S_4(SPh)_2Cl_2]$. From the possible equilibria in solution between various mixed ligand clusters (1) $[Fe_4S_4SPhCl_3]^{2-} + [Fe_4S_4(SPh)_3Cl]^{2-} \rightleftarrows 2[Fe_4S_4(SPh)_2Cl_2]^{2-}$ and (2) $[Fe_4S_4(SPh)_4]^{2-} + [Fe_4S_4Cl_4]^{2-} \rightleftarrows 2[Fe_4S_4(SPh)_2Cl_2]^{2-}$. The $[Fe_4S_4(SPh)_2Cl_2]^{2-}$ anion readily precipitates out as a Ph_4P^+ salt. That equilibrium 2 exists in solution and favors formation of II also is evident in the electronic spectrum of an equimolar mixture of $[Fe_4S_4Cl_4]^{2-}$ and $[Fe_4S_4(SPh)_4]^{2-}$. The electronic spectrum (Figure 6) indicates that in this mixture the major component is the $[Fe_4S_4(SPh)_2Cl_2]^{2-}$ cluster which forms in ~76% yield.

Adequate evidence that the $(Ph_4P)_2[Fe_4S_4(SPh)_2Cl_2]$ is not an equimolar mechanical mixture of Ph_4P^+ salts of $[Fe_4S_4(SPh)Cl_3]^{2-}$ and $[Fe_4S_4(SPh)_3Cl]^{2-}$ or $[Fe_4S_4(SPh)_4]^{2-}$ and $[Fe_4S_4Cl_4]^{2-}$ is found in the solid-state characterization of this compound. The X-ray powder pattern of $(Ph_4P)_2[Fe_4S_4(SPh)_2Cl_2]$ is different than that of either $(Ph_4P)_2(Fe_4S_4Cl_4)$ or $(Ph_4P)_2[Fe_4S_4(SPh)_4]$.

The final proof of identity is available in the results of a X-ray diffraction single-crystal structure determination[32,33] of the $(Ph_4P)_2[Fe_4S_4(SPh)_2Cl_2]$ salt. The molecular structure of the anion (Figure 7) contains the Fe_4S_4 cubic core with two chloride and two thiophenolate terminal ligands.

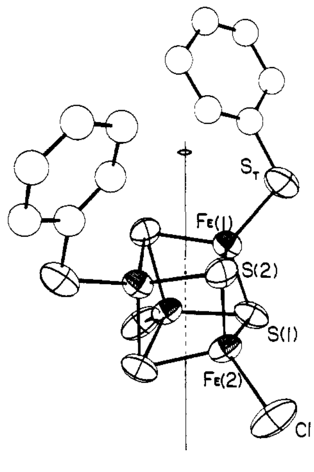

Figure 7. Structure of the $[Fe_4S_4Cl_2(SPh)_2]^{2-}$ anion[32] showing 50% probability ellipsoids for the non-carbon atoms. Distances: Fe_i–Fe_i i = 1, 2.756 (4); i = 2, 2.774 (4); Fe_i–Fe_j, 2.728 (4) Å and 2.745 (4) Å; Fe_i–S_i, i = 1, 2.298 (6); i = 2, 2.301 (6); Fe_i–S_j, range from 2.258 (5) to 2.281 (5) Å with a mean value of 2.27 (1) Å; Fe(1)–S_t, 2.265 (6) Å; Fe(2)–Cl(1), 2.211 (5) Å. Angles: Fe(1)–S(2)–Fe(1), 74.8(2)°; Fe(2)–S(1)–Fe(2), 75.1 (2)°; Fe_i–S_b–Fe_j, range from 73.1 (2) to 73.9 (2)° with a mean value of 73.5 (3)°; S(2)–Fe(1)–S(2), 102.4 (3)°; S(1)–Fe(2)–S(1), 102.1 (3)°; S_i–Fe–S_j, range from 104.3 (3) to 106.7 (3)° with a mean value of 105.1 (9)°.

The reactions of $[Fe_4S_4(SPh)_2Cl_2]^{2-}$ with KSPh or PhCOCl in 1:2 molar ratios to afford either $[Fe_4S_4(SPh)_4]^{2-}$ or $[Fe_4S_4Cl_4]^{2-}$ in excellent yields forecast the possible utility of II as a convenient reagent for the syntheses of various mixed-ligand cubanes. Analogous reactions with KSR or PhCOCl have been reported previously[18] by Holm and co-workers for either the $[Fe_4S_4Cl_4]^{2-}$ or the $[Fe_4S_4(SPh)_4]^{2-}$ clusters. In these reactions the $[Fe_4S_4(SR)_4]^{2-}$ or $[Fe_4S_4Cl_4]^{2-}$ clusters respectively were obtained in very good yields.

In reactions, where the BzSSSBz to I molar ratio is >4, complete oxidation of the phenyl mercaptides in I occurs and the tetrachloro cubane, $[Fe_4S_4Cl_4]^{2-}$, is isolated in very good yields. This complex anion has been obtained and structurally characterized previously.[18] The synthesis of $[Fe_4S_4Cl_4]^{2-}$ from BzSSSBz and $[Fe_4(SPh)_6Cl_4]^{2-}$ is more efficient in CH_3CN/DMF mixtures where the maximum yields were obtained with a 4:1 BzSSSBz/I molar ratio. By contrast the maximum yield of $[Fe_4S_4Cl_4]^{2-}$ by the same reaction in CH_3CN is realized with an 8:1 BzSSSBz/$[Fe_4(SPh)_6Cl_4]^{2-}$ molar ratio. The synthesis of $[Fe_4S_4Cl_4]^{2-}$ from $[Fe_4(SPh)_6Cl_4]^{2-}$ and BzSSSBz in a CH_3CN/DMF mixture resembles the synthesis of $[Fe_4S_4(SPh)_4]^{2-}$ from elemental sulfur and $[Fe_4(SPh)_{10}]^{2-}$ according to the reaction reported recently by Holm and co-workers.[10,16]

$$[Fe_4(SPh)_{10}]^{2-} + 4S \rightarrow [Fe_4S_4(SPh)_4]^{2-} + 3PhSSPh$$

Electrochemical Studies. The cyclic voltammetry of $[Fe_4S_4(SPh)_2Cl_2]^{2-}$ in either CH_3CN or DMF solutions shows a *clean single* potential for the 2-/3- couple, less negative than the corresponding potential for $[Fe_4S_4(SPh)_4]^{2-}$ by 5–10 mV. Under the same electrochemical conditions the 2-/3- couple for $[Fe_4S_4Cl_4]^{2-}$ is observed at even less negative potentials by approximately the

---

(32) (a) Crystal data for $(Ph_4P)_2Fe_4S_4Cl_2(SPh)_2$: cell dimensions a = 13.08 Å b = 21.22 Å, c = 21.34 Å, $\alpha = \beta = \gamma$ 90°, space group *Pbcn*, d_{obsd} = 1.48 g/cm^3, d_{calcd} = 1.47 g/cm^3. The $[Fe_4S_4(SPh)_2Cl_2]^{2-}$ anions located on the crystallographic twofold symmetry axes at 0, y, $^1/_4$, 0, y, $^3/_4$, $^1/_2$, $^1/_2 + y$, $^1/_4$, and $^1/_2$, $^1/_2 - y$, $^3/_4$. The structure was solved on the basis of a minimum set of reflection data (an octant of the reflection sphere), and the present value of R is 10%. A collection of a full sphere of reflection data is currently underway. The new data will be used in the final refinements of the structure which will be published in a forthcomming publication.[33]

(33) Kanatzidis, M.; Baenziger, N. C.; Coucouvanis, D., manuscript in preparation.

Table VI. Peak Potentials[a] for the Couples $[Fe_4S_4(SPh)_{4-n}X_n]^{2-/3-}$

	E_p, V	$E_{pc} - E_{pa}$, mV	i_{pc}/i_{pa}	concn, M
$[Fe_4S_4(SPh)_4]^{2-}$	−1.05	86	0.95	1.6×10^{-3}
$[Fe_4S_4(SPh)_2Cl_2]^{2-}$	−0.95	100	0.87	1.2×10^{-3}
$[Fe_4S_4Cl_4]^{2-}$	−0.87	109	0.89	1.0×10^{-3}
	In CH_3CN			
$[Fe_4S_4(SPh)_4]^{2-}$	−0.90	72	0.96	5×10^{-4}
$[Fe_4S_4(SPh)_2Cl_2]^{2-}$	−0.85	168	0.88	1.7×10^{-3}
$[Fe_4S_4Cl_4]^{2-}$	−0.72	133	0.89	1.2×10^{-3}

[a] Solutions were 0.1 M in tetra-*n*-butylammonium perchlorate. Potentials are reported vs. a saturated calomel electrode. In all measurements the scan rate was 200 mV/s.

same 5–10-mV increments (Table VI). The values for the 2^-–3^- couples for the $[Fe_4S_4(SPh)_4]^{2-}$ and $[Fe_4S_4Cl_4]^{2-}$ clusters in *N*-methyl-2-pyrrolidinone vs. SCE electrode at −1.04 and −0.85 V, respectively,[34] compare very favorably with corresponding values we have obtained in DMF at −1.05 and −0.87 V. The deviations of the anodic–cathodic peak separations ($|E_{pa} - E_{pc}|$) from the theoretical 0.059 mV may indicate the absence of strict electrochemical reversibility. However, the cathodic to anodic peak current ratios, (i_{pc}/i_{pa}) (Table VI) are all very close to 1 and suggest effective chemical reversibility.

Mixed chloro mercaptido "cubanes" of the type $[Fe_4S_4(SR)_{4-n}X_n]^{2-}$ have been reported previously[34] as species present in $[Fe_4S_4(SR)_4]^{2-}/C_6H_5COCl$ reaction mixtures. Possible difficulties encountered in the isolation of any such species are apparent in the statement: "...the roughly statistical distribution of species presumably precludes isolation of a pure salt of any one such species...".[34]

The utility of $[Fe_4S_4(SPh)_2Cl_2]^{2-}$ as a precursor for the synthesis of "mixed" mercaptido clusters of the types $[Fe_4S_4(SR)_2(SR')_2]^{2-}$ or $[Fe_4S_4(SR)_2(L)_2]^{n-}$ is at present under investigation.

Acknowledgment. This work has been generously supported by a grant from the National Institute of Health (No. GM-26671-02). The computer expenses have been covered by grants from the University of Iowa Graduate College.

Registry No. I, 80765-11-3; II, 80939-30-6; III, 80765-12-4; $(Ph_4P)_2[Fe_4(SPh)_6Br_4]$, 80789-26-0; $(Ph_4P)_2[Fe_4S_4(SPh)_4]$, 80765-13-5; $[Fe_4(S\text{-}p\text{-tol})_6Cl_4]^{2-}$, 80765-08-8; $(Ph_4P)_2Fe(SPh)_4$, 57763-34-5; BzSSSBz, 6493-73-8; BzSH, 100-53-8; SCl_2, 10545-99-0; PhCOCl, 98-88-4.

Supplementary Material Available: Tables of observed structure factors for $(Ph_4P)_2[Fe_4(SPh)_6Cl_4]$ (32 pages), final atomic positional and thermal parameters for the phosphorus and carbon atoms of the cations and the anion, weighted least-squares planes and dihedral angles (38 pages). Ordering information is given on any current masthead page.

---

[34] Johnson, R. W.; Holm, R. H. *J. Am. Chem. Soc.* **1978**, *100*, 5338.

Syntheses and Electronic Structures of Decamethylmetallocenes

J. L. Robbins,[*] N. Edelstein, B. Spencer,[†] and J. C. Smart[‡]

Contribution from the Materials and Molecular Research Division, Lawrence Berkeley Laboratory, University of California, Berkeley, California 94720.

Received June 11, 1981

Abstract: The syntheses of the $(Me_5Cp)_2M$ (M = Mg, V, Cr, Co, and Ni) and $[(Me_5Cp)_2M]PF_6$ (M = Cr, Co, and Ni) compounds are described. In addition, a preparative route to a novel, dicationic decamethylmetallocene, $[(Me_5Cp)_2Ni](PF_6)_2$, is reported. Physical measurements indicate that all the above compounds are D_{5d} or D_{5h} decamethylmetallocenes with low-spin electronic configurations. The decamethylvanadocene cation is apparently coordinatively unsaturated. A paramagnetic acetonitrile complex, $[(Me_5Cp)_2V(NCCH_3)]PF_6$, and a diamagnetic dicarbonyl derivative, $[(Me_5Cp)_2V(CO)_2]PF_6$, of the cation can be prepared, but pure $[(Me_5Cp)_2V]PF_6$ has not been isolated. Cyclic voltammetry studies verify the reversibility and the one-electron nature of the $(Me_5Cp)_2M \rightleftharpoons [(Me_5Cp)_2M]^+$ (M = Cr, Fe, Co, and Ni) and $[(Me_5Cp)_2Ni]^+ \rightleftharpoons [(Me_5Cp)_2Ni]^{2+}$ redox reactions and show that the neutral decamethylmetallocenes are much more easily oxidized than their metallocene counterparts due to the electron-donating properties of the methyl groups. Magnetic susceptibility and EPR studies indicate the following ground-state assignments for the paramagnetic decamethylmetallocenes: ${}^4A_{2g}[e_{2g}{}^2a_{1g}{}^1]$ for the 15-electron compounds $(Me_5Cp)_2V$ and $[(Me_5Cp)_2Cr]^+$, ${}^3E_{2g}[e_{2g}{}^3a_{1g}{}^1]$ for the 16-electron compounds $(Me_5Cp)_2Cr$ and $[(Me_5Cp)_2Mn]^+$, ${}^2E_{2g}[e_{2g}{}^3a_{1g}{}^2]$ for the 17-electron compound $[(Me_5Cp)_2Fe]^+$, ${}^2E_{1g}[e_{2g}{}^4a_{1g}{}^2e_{1g}{}^1]$ for the 19-electron compounds $(Me_5Cp)_2Co$ and $[(Me_5Cp)_2Ni]^+$, and ${}^3A_{2g}[e_{2g}{}^4a_{1g}{}^2e_{1g}{}^2]$ for the 20-electron compound $(Me_5Cp)_2Ni$. The UV–visible absorption spectra of the 15-, 18- and 20-electron decamethylmetallocenes are also reported. Assignments are proposed for the absorptions due to d–d transitions, and a ligand-field analysis is used to derive the ligand-field splitting parameters Δ_1 and Δ_2 and the Racah electron repulsion parameter *B*. Comparison of these parameters with those previously reported for the isoelectronic Cp_2M compounds shows the net ligand-field splitting and *B* are larger in the permethylated compounds. The increased value of *B* indicates greater electron density at the metal center.

Since the discovery[1] and structural characterization[2,3] of ferrocene (η^5-$(C_5H_5)_2Fe$ or Cp_2Fe) in the early 1950s, at least one cyclopentadienyl derivative of every main group and transition metal, as well as most f-block metals, has been prepared and characterized.[4–6] A large number of monoalkyl- and monoaryl-substituted cyclopentadienyl metal compounds have also been

---

[*] To whom correspondence should be sent at Exxon Research and Engineering Co., Linden, NJ 07036.

[†] Chemistry Department, Beloit College, Beloit, WI 53511.

[‡] Solar Energy Research Institute, Golden, CO 80401.

(1) Kealy, T. J.; Pauson, P. L. *Nature* (*London*) **1951**, *168*, 1039–1040.

(2) Wilkinson, G.; Rosenblum, M.; Whiting, M. C.; Woodward, R. B. *J. Am. Chem. Soc.* **1952**, *74*, 2125–2126.

(3) Fischer, E. O.; Pfab, W. *Z. Naturforsch.* **1952**, *74*, 2125–2126.

(4) Coates, G. E.; Green, M. L. H.; Wade, K. "Organometallic Compounds", 3rd ed.; Methuen: London, 1967.

0002-7863/82/1504-1882$01.25/0 © 1982 American Chemical Society